8-5-2021

# Molten-Salt-Assisted Annealing for Making Colloidal ZnGa2O4:Cr Nanocrystals with High Persistent Luminescence

Bhupendra B. Srivastava
*The University of Texas Rio Grande Valley*

Santosh K. Gupta

Swati Mohan
*The University of Texas Rio Grande Valley*

Yuanbing Mao



## Recommended Citation

Srivastava, Bhupendra B., et al. "Molten-Salt-Assisted Annealing for Making Colloidal ZnGa2O4: Cr Nanocrystals with High Persistent Luminescence." Chemistry–A European Journal 27.44 (2021): 11398-11405. https://doi.org/10.1002/chem.202101234

**Author Manuscript**

**Title:** Molten Salt Assisted Annealing for Making Colloidal ZnGa2O4:Cr Nanocrystals with High Persistent Luminescence

**Authors:** Bhupendra B. Srivastava; Santosh K. Gupta; Swati Mohan; Yuanbing Mao



**To be cited as:** 10.1002/chem.202101234

**Link to VoR:** https://doi.org/10.1002/chem.202101234

# Molten Salt Assisted Annealing for Making Colloidal $ZnGa_2O_4$:Cr Nanocrystals with High Persistent Luminescence

Bhupendra B. Srivastava[1*], Santosh K. Gupta[2,3], Swati Mohan[1], and Yuanbing Mao[4*]

[1]Department of Chemistry, University of Texas Rio Grande Valley, 1201 West University Drive, Edinburg, Texas 78539, USA

[2]Radiochemistry Division, Bhabha Atomic Research Centre, Trombay, Mumbai400085, India

[3]Homi Bhabha National Institute, Anushaktinagar, Mumbai400094, India

[4]Department of Chemistry, Illinois Institute of Technology, 3101 South Dearborn Street, Chicago, IL 60616, USA

* To whom correspondence should be addressed. Electronic mails: bhupendra.srivastava@utrgv.edu (BBS) and ymao17@iit.edu (YM).

**Abstract:**

Persistent luminescent nanocrystals (PLNCs) in sub-10 nm domain are considered most fascinating inventions in lighting technology owing to their excellent performance in anti-counterfeiting, luminous paints, bioimaging, security applications, etc. Further improvement of persistent luminescence (PersL) intensity and lifetime is needed to achieve the desired success while keeping uniform sub-10 nm size of PLNCs. In this work, we have introduced the concept of molten salt confinement to thermally anneal as-synthesized $ZnGa_2O_4:Cr^{3+}$ (ZGOC) colloidal NCs (CNCs) in a molten salt media at 650$^o$C for the first time. This method led to significantly monodispersed and few agglomerated NCs with much improved photoluminescence (PL) and PersL intensity without much size growth of the pristine CNCs. Other strategies, such as: (i) thermal annealing, (ii) overcoating, and (iii) core-shell strategy, have also been tried to improve PL and PersL but we could not achieve improvement in their PL and PersL simultaneously. Moreover, directly annealing of the CNCs in air without the molten salt assistance could significantly improve both PL and PersL but lead to particle heterogeneity and aggregation, which are highly unsuitable for in vivo imaging. We believe this work provides a novel strategy to design PLNCs with high PL intensity and long PersL duration without losing their nanostructural characteristics, water dispersibility and biocompatibility.

**Keywords:** Molten Salt; Persistent Luminescence; $ZnGa_2O_4:Cr^{3+}$; Nanocrystals

## Introduction

$ZnGa_2O_4:Cr^{3+}$ (ZGOC) has been studied in the realm of scientific research because its extraordinary persistence luminescence property in near-infrared (NIR) region has rendered various applications which touches day to day human life.[1,2,3,4,5,6,7,8] Some of the most rewarding applications include optical imaging of tumors and grafted cells,[9,10,11] security and emergency signages,[12] gene silencing in cancer cells and cancer therapy,[13,14] information storage,[15] etc. With no doubt, ZGOC is one of the best performing and rechargeable NIR PersL phosphors reported so far.[16] However for many of its applications to be realized at commercial stage, high photoluminescence (PL) emission output and long persistent luminescence (PersL) duration is utmost required.[3,6,17]

In general, to improve the efficacy of ZGOC as a NIR PersL phosphor, thermal treatment at ~750ºC, grinding/laser ablation, or other tedious treatments are needed for pre-formed ZGOC nanocrystals (NCs) while these processes mostly result in particle growth and high level of agglomeration.[16,18,19,20] Driven by the same motivation, co-doping strategy has also been explored which has shown improved PL and PersL of ZGOC co-doped with $W^{6+}$, $Ge^{4+}/Sn^{4+}$, $Bi^{3+}$, boron, $Si^{4+}$ ions, etc.[12,14,21,22,23,24] EDTA etching has also seemed to enhance the PersL longevity of ZGOC.[15] However, in the aforementioned literature articles, ZGOC was either in bulk form or if nanoparticles were used then they were either partially agglomerated or had polydispersity in size. Similarly, Hussen *et al.* enhanced PL intensity of ZGOC by annealing them at 1000ºC but increased its particle size from 12 to 31 nm which is highly undesirable.[25] On the similar ground, annealing ZGOC phosphor at 800ºC enhanced its PL intensity by an order of six but there was a large growth of particle size along with particle aggregation.[26]

Here we want to mention that maintaining the size and shape of ZGOC nanoparticles is utmost important as:(i) When ZGOC is synthesized in nanodomain, higher PL intensity is shown compared to its agglomerated form (agglomerated NCs/microcrystals).[25] (ii) For optical imaging and information applications, sub-10 nm particles are ideal as they can easily percolate through cells for bioimaging while exhibiting good dispersity in biological media and displaying negligible photobleaching.[27] There have been a few reports wherein researchers have used synthetic modifications to get rid of high agglomeration and heterogeneity of ZGOC NCs. Han and his group synthesized ZGOC NCs in the pores of mesoporous $SiO_2$ nanoparticles at temperature less than 600ºC, which displayed excellent PersL performance.[16] Jiang *et al.* improved blood compatibility

by avoiding agglomeration of ZGOC NCs upon surface functionalization with hydrophilic polyethylene glycol (PEG) polymers for optical imaging applications.[10] Similarly silica coating on Sn co-doped $ZnGa_2O_4:Cr^{3+}$ were performed on 15 nm NCs which showed improved PersL by a factor of 13.5.[28] There have been reports on controlling the size of ZGOC NCs by using ethylene diamine as reactant and surfactant ligand.[29] Moreover, to achieve high PL output and long PersL duration from ZGOC NCs, our group has successfully developed a bi-phasic route for the first time to synthesize sub-10 nm ZGOC NCs.[3] More recently, to improve both PL intensity and PersL duration of ZGOC NCs, we have also developed a different synthetic approach by altering several synthetic parameters such as (i) controlled urea precipitation, (ii) adjusting the Zn/Ga precursor ratio, and (iii) the addition of ammonium nitrate.[6] Similarly, Teston et al. synthesized ZGOC NCs as small as 6 nm using a microwave irradiation aided non-aqueous sol–gel process.[30] There is another report of sub-10 nm ZGOC NCs by aqueous phase synthesis, where the authors used a hydrothermal method with $NH_4OH$(aq) to synthesizing ZGOC and tuned the size of the NCs by modulating the precursor composition.[2]

However, in all these reports, monodisperse (similar size and shape), non-agglomerated and nanosized ZGOC with high PL output and long PersL still have not been fully achieved yet. It is believed that homogenous and monodispersed PLNCs have less scattering of excited and emitted photon, which could endow higher PL and PersL output by d-d transitions of $Cr^{3+}$ ion from ZGOC NCs. At the same time, the extent of electron hole overlapping integral would be higher for sub-10 nm ZGOC NCs coupled with monodispersity and homogeneity, and hence higher luminescence intensity can be harnessed. In our understanding, the main issue for the synthesized ZGOC NCs is that the synthesis techniques, i.e. hydrothermal, biphasic hydrothermal, and sol-gel methods, actually give less control on particle size and shape compared to the popular colloidal technique for NCs.[31,32,33,34] In this context, zinc gallate (ZGO) colloidal NCs (CNCs) synthesized by controlled growth have added advantages of well-defined size, shape and monodispersity which are highly essential for device fabrications, information storage, and biomedical applications with favorable PL and PersL features.[35,36,37,38]

As far as ZGOCNCs are concerned, a few studies have reported on undoped and $Eu^{3+}$/$Tb^{3+}$ doped ZGO CNCs pertaining to light emitting phosphors but there is no report on ZGOC CNCs.[39,40] Generally speaking, to get desirable PersL properties from ZGOC NCs, one need to anneal them at a high temperature range of 650-750$^{o}$C which leads to particle agglomeration and size non-

uniformity as reported by several research groups earlier.[16,19,20,25,26] To overcome this obstacle, in the current study, we have introduced a new approach with a molten salt confinement concept to thermally anneal as-synthesized ZGOC CNCs in a molten salt media of $NaNO_3$ + $KNO_3$ at 650$^o$C for the first time. In one of our previous work, we annealed pyrochlore nanoparticle annealing in a molten salt which led to enhanced emission intensity and excited state lifetime.[41] The molten salt assisted process provides added advantages by offering not only a high temperature environment needed for annealing but also a unique reaction medium with high ionic strength.[42] The molten salt as a medium provides enhanced contacts for reactant and allows controlled particle growth.[43,44] Li et al. used heat treatment assisted molten salt strategy to improve the electrochemical performance of Li-rich Mn-based layered oxide (LMRO) assembled microspheres.[45] Previous results have shown that molten salt synthesis of spinel leads to controlled growth in size and shape of nano materials.[46] To make ZGOC CNCs much more commercially viable in the area of information storage and bioimaging, this work facilitates the need to improve the deep red PersL intensity and duration of ZGOC CNCs without losing their advantages of nanometer size, biocompatibility and monodispersity by annealing them in a molten salt. Our study demonstrated that the molten salt assisted annealing of pre-formed ZGOC CNCs at 650$^o$C led to monodisperse and non-agglomerated NCs without much particle size change while, equally important, endowed improved PL and PersL intensity. For readers to have convenient comparison of advantages of these methods, we have compiled PersL performance of different sub-10 nm ZGOC NCs along with their synthesis protocols in Table S1.

## Experimental

**Materials:** Zinc acetylacetonate hydrate ($Zn(acac)_2 \cdot xH_2O$, 99.995%), gallium acetylacetonate ($Ga(acac)_3$, 99.99%), chromium (III) acetylacetonate ($Cr(acac)_3$, 99.99%), oleic acid (technical grade, 90%), octadecene-1 (ODE, technical grade, 90%), oleylamine (technical grade, 70%), $NaNO_3$ (≥ 99.0%), $KNO_3$ (≥ 99.0%), sodium trifluroacetate (98%), yttrium trifluoroacetate (99%), and chloroform (anhydrous, ≥ 99%) were purchased from Sigma Aldrich. Acetone (≥ 99.5%) was purchased from Fisher Scientific. All chemicals were of analytical grade reagents and used directly without further purification in this work.

**Colloidal Synthesis of ZGOC CNCs**

In a typical one-pot colloidal synthesis process of the ZGOC CNCs, firstly 0.5 mmol of $Zn(acac)_2 \cdot xH_2O$, 1.0 mmol of $Ga(acac)_3$, 0.01 mmol of $Cr(acac)_3$, 1 mL of oleic acid and 6 grams of ODE were taken into a 50 mL three-necked flask and heated at 120°C for 1 hour under vacuum. After this step, the vacuum was released, and the reaction mixture was further heated to 300°C under an argon atmosphere for 30 minutes to further grow the ZGOC CNCs. Aliquots were taken at different time intervals for PL and TEM characterization. After 30 minutes, the system was cooled to room temperature after removing heating. The cooled reaction mixture was further purified with chloroform/acetone as the solvent/antisolvent mixture, which resulted in an as-purified mixture with gluey white color texture. We stored this mixture for further post-synthesis processes as described below. The experimental setup for the colloidal synthesis of the ZGOC CNCs is shown in Figure S1.

**Over-Coating of ZGOC CNCs with ZGO**

As-purified ZGOC CNCs (approx. 500 mg) were transferred into a 50 mL three-necked flask and dispersed in 5mL ODE and was heated to 120°C for 1 hour under vacuum. After this step, the vacuum was released, and the reaction mixture was further heated to 250°C under an argon atmosphere. At this temperature 0.5 mmol of $Zn(acac)_2 \cdot xH_2O$, 1.0 mmol of $Ga(acac)_3$, stock in 5 mL ODE was degassed and injected. Upon injection temperature got reduced to 220°C and it further annealed at this temperature for 30 more minutes. After that the system was cooled to room temperature by removing the heating.

**Coating ZGOC CNCs with a $NaYF_4$ Shell**

As-purified ZGOC CNCs (approx. 500 mg) were transferred into a 50 mL three-necked flask and dispersed in 5 mL ODE, and then 1 mmol of sodium trifluoroacetate, 1 mmol of yttrium trifluoroacetate and 2 mL oleylamine were added. The obtained mixture in the three-necked flask was heated to 120°C for 1 hour under vacuum. After this step, the vacuum was released, and the reaction mixture was further heated to 300°C under an argon atmosphere and kept for 30 minutes at this temperature. After that the system was cooled to room temperature by removing the heating. The cooled reaction mixture was further purified with a chloroform/acetone mixture as the solvent/antisolvent. The product was denoted as ZGOC:$NaYF_4$ core-shell NPs.

**Molten Salt Assisted Annealing of ZGOC CNCs**

As-purified ZGOC CNCs (approx. 500 mg) was also directly annealed at 650°C for 6 h with a ramp-up rate of 15°C $min^{-1}$ and cooling-down rate of 10°C $min^{-1}$ with the addition of 60 mmol of

$NaNO_3$ and 60 mmol of $KNO_3$ as the molten salt. The annealed product was then also washed several times with deionized water and dried in an oven at 60ºC overnight. The sample was denoted as ZGOC MSS-650.Choice of annealing time and temperature was dictated by the optimum condition which can yield NCs with optimum size, low or no aggregation, low surface defects and ideal crystallinity.[43] The MSS synthesis temperature (650°C) was above the eutectic temperature (230–320°C) of the added $NaNO_3$-$KNO_3$ salts and below their decomposition temperatures (~700°C) to serve as the molten media.[47]

**Direct Thermal Annealing of ZGOC CNCs at 650ºC**

As-purified ZGOCCNCs (approx. 500 mg) was also directly annealed at 650ºC for 6 h with a ramp-up rate of 15ºC $min^{-1}$ and cooling-down rate of 10ºC $min^{-1}$ without the addition of $NaNO_3$ and $KNO_3$ as the molten salt. The annealed product was then also washed several times with deionized water and dried in an oven at 60ºC overnight. The sample was denoted as ZGOC HT-650.

**Instrumentation**

Powder X-ray diffraction (XRD) patterns of the four products described above were taken with a Bruker D8 ADVANCE X-ray diffractometer with Cu $K_{\alpha 1}$ radiation ($\lambda$ = 0.15406 nm). XRD data were collected by utilizing a scanning mode of 2θ ranging from 25° to 70° with a scanning step size of 0.04° and a scanning rate of 2.0° $min^{-1}$. Transmission electron microscopic (TEM) and high-resolution TEM (HRTEM) images were recorded using a Hitachi HF 3300 TEM/STEM system. PL emission and excitation spectra were recorded using an Edinburgh Instrument FLS 980 fluorimeter system with a steady state xenon lamp source. PersL data were also recorded on the Edinburgh Instrument FLS 980 fluorometer system on a kinetic scan mode by exciting the samples for 5 minutes at 256 nm and then measuring the decay of 696 nm emission.

## Result and discussion

### XRD

XRD patterns of the ZGOC CNCs, HT-650, and MSS-650 samples (Figure 1) displayed the peaks corresponding to (hkl) planes of (311), (440), (511), (422), (400), and (220), which completely match with the $ZnGa_2O_4$ crystallographic phase having standard ICDD file of #86-0415 (space group: Fd-3m). It confirmed the formation of phase pure spinel cubic crystalline structure of ZGOC as $Zn^{2+}$ and $Ga^{3+}$ stabilize in $ZnO_4$ tetrahedra and $GaO_6$ octahedral, respectively, and $Cr^{3+}$

doping ions (ionic radius with coordination number (CN) of 6 = 0.63 Å) can easily substitute $Ga^{3+}$ ions (ionic radius with CN of 6 = 0.62 Å). Based on the Debye Scherer equation, the calculated crystallite size of the ZGOC CNCs was ~5.5 nm. Compared with the XRD pattern of the ZGOC CNCs, that of the ZGOC HT-650 sample did not change much in terms of peak profile but there was alteration in full width half maxima (FWHM) of XRD peaks. Specifically, the FWHM of the XRD peaks became smaller significantly, which suggested the increase of the particle size to 21.5 nm as confirmed by the calculation using the Debye Scherer equation. The same observation was ascribed to crystal growth of ZGOC NCs after annealed at 750ºC through Ostwald ripening wherein larger particles are more energetically favorable compared to smaller ones.[48] On the other hand, there was not much change in the FWHM of the ZGOC MSS-650 NCs suggesting that the ZGOC CNCs did not grow or were etched significantly. The calculated nanocrystallite size of the ZGOC MSS-650 NCs was ~6.2 nm, which was close to that of the pristine ZGOC CNCs.

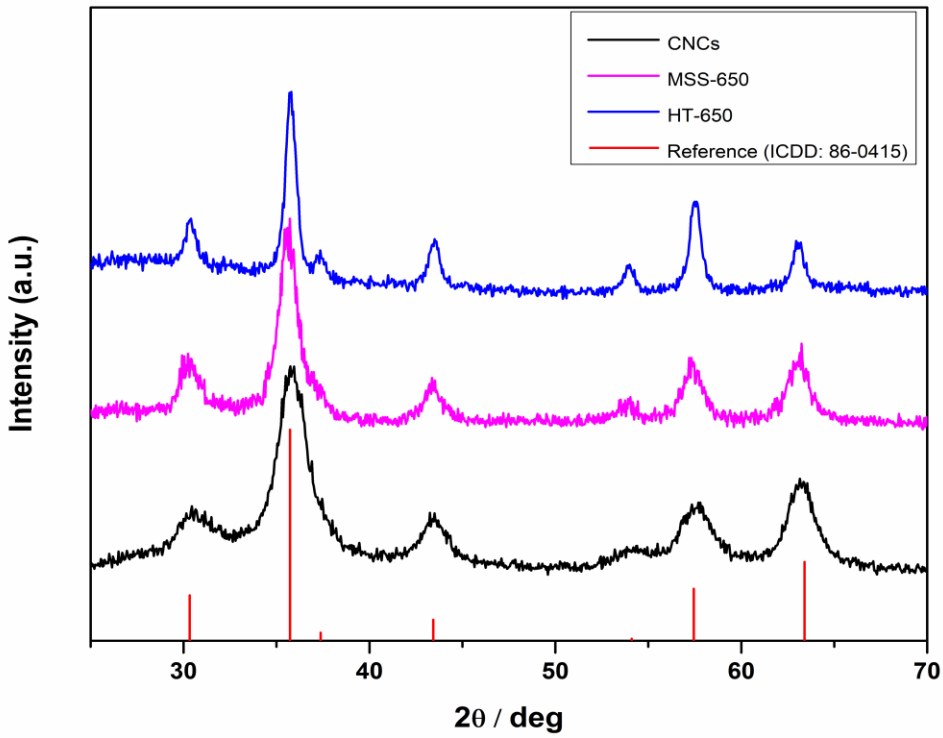


**Figure 1.** XRD patterns of the ZGOC CNCs, MSS-650 and HT-650 along with the standrard JCPDS paterern of ZGO (#86-0415).

**TEM**

TEM images under different magnifications of the ZGOC CNCs, MSS-650 and HT-650 NCs were shown in Figures 2a, 2b and 2c, respectively. Specifically, TEM images of the ZGOC CNCs (Figure 2a) clearly showed the formation of ultra-small and highly monodispersed ZGOC NCs in the range of 4-5 nm without any aggregation or agglomerations. The relevant HRTEM image displayed the appearance of well-defined lattice fringes of ZGOC CNCs suggesting not coalesced particles.[40]

Not much variation in the particle size was observed upon thermal treatment of the ZGOC CNCs in the $NaNO_3$-$KNO_3$ molten salt (Figure 2b). Even after the annealing in the molten salt, the ZGOCMSS-650 NCs only had slight aggregation when dispersed in water due to the absence of any surface functionalization ligand (Figure 2b, left panel). The ZGOC MSS-650 NCs allowed better dispersion in water after 5 minutes sonication owing to their small size and non-agglomeration. Large aggregates of the ZGOC CNCs formed after direct thermal treatment of them in the absence of molten salt assistance (Figure 2c). The direct thermal annealing raised the particle size of the ZGOC CNCs from ~5 nm to ~21.5 nm for the ZGOC HT-650 NCs with large degree of aggregation. Even after 10 min sonication, the ZGOC HT-650 NCs were not dispersed in water. Their particles were clustered together when added in water. We also treated the ZGOC HT-650 NCs with oleic acid along with further sonication for better dispersion. Unlike the ZGOC MSS-650 NCs, these ZGOC HT-650 NCs were still unable to be dispersed and showed aggregation due to their large particle size ascribed above to crystal growth assisted by Ostwald ripening. When no molten salt was added, the high temperature annealing for the ZGOC HT-650 NCs proceeded similar to solid state reaction wherein the rate determining step was particle diffusion and it happened at the interface of two solid particles at the solid-solid interface.

Moreover, the ZGOC CNCs and MSS-650 NCs had different dispersion nature in different solvents. Our experiments showed that the ZGOC CNCs were highly dispersible in organic solvents such as hexane, toluene, and chloroform. On the other hand, the ZGOC MSS-650 NCs were dispersible in water after 10 min sonication and in organic solvents including chloroform, toluene, and hexane after further oleic acid treatment.

**Unique role of molten salt in generating size-controlled aggregate-free NCs**

The added molten salts efficiently covered the surface of the as-formed ZGOC CNCs during the post-synthesis annealing treatment, which inhibited any kind of neck formation between the ZGOC CNC particles leading to extremely low or no agglomeration.[43] This surface protection also led

to the formation of highly homogenous and well-defined NCs with uniform particle size distribution. It is commonly believed that extended heating of nanomaterials assisted with or without salt fluxes would lead to crystal growth via Ostwald ripening. Our interesting observation of the stabilization of the as-synthesized ZGOC CNCs in the $NaNO_3$-$KNO_3$ molten salt without much particle growth nor any coalescence or aggregation is difficult to be explained by conventional electrostatic and steric mechanism. Stabilization of aggregation-free CNCs in any solvent requires that the Columbic repulsion among NCs could overcome the van der Waals force.[49] On the other hand, for high dielectric solvent such as water, the general theory of electrostatic interactions work relatively well in stabilizing CNCs without any aggregations.[50,51] The refractive index of the ZGOC NCs is higher than the $NaNO_3$-$KNO_3$ molten salt, therefore, refractive index matching cannot be the sole criteria to overpower van der Waals attraction. Here the role of the high charge density of molten salts comes to play a big role. It leads to strong electrostatic screening producing short-ranged Coulomb repulsion and causes weakening of van der Waals attraction.[52] As predicted by theoretical modeling, the formation of long range charge density oscillation in molten salts provided by the surface bound layer prevents any kind of coalescence or aggregation around reactant species, i.e. the ZGOC CNCs by the inorganic $KNO_3$-$NaNO_3$ molten salt solvent in this work.[38] Moreover, the low NC to molten salt ratio gave large separation between the ZGOC NCs to slow down or even prevent their Ostwald ripening for particle growth. The schematic of molten salt assisted annealing of the ZGOC CNCs without any substantial crystal growth or aggregation is shown in Figure S2.

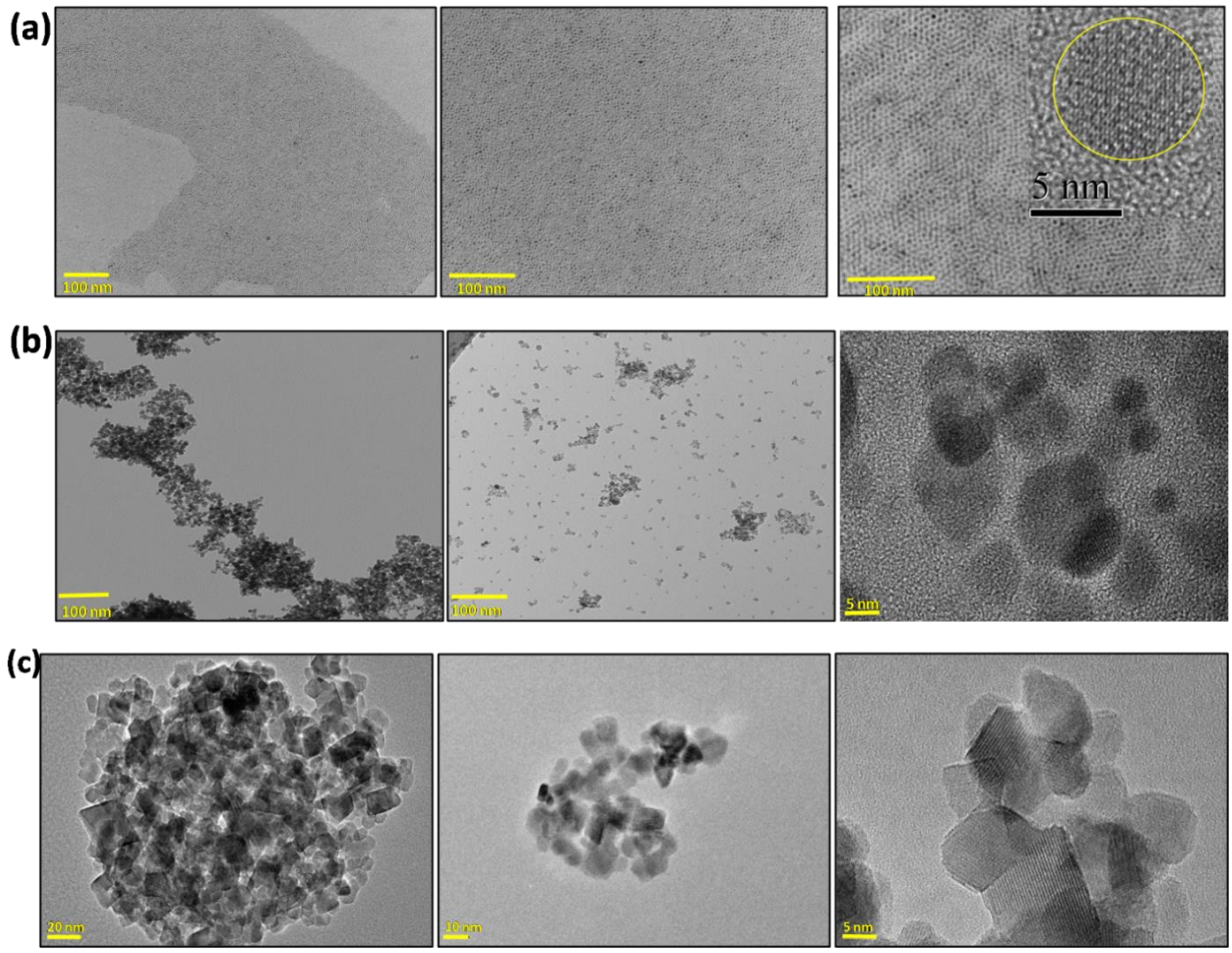


**Figure 2.** TEM images of the ZGOC samples: (a) The CNCs dispersed in chloroform with the inset in the rightmost panel showing the HRTEM image of an individual CNC. (b) The MSS-650 NCs dispersed in water (left panel), after 5 minutes sonication in water (middle panel), and the HRTEM image after dispersion in water. (c) The HT-650 NCs dispersed in water at different magnifications.

**Luminescence spectroscopy**

As reported on the literature, annealing ZGOC samples at high temperatures, normally around 700$^{o}$C, has been widely employed to enhance their PL intensity and PersL intensity and duration. It is believed that annealing them at high temperatures leads to faster diffusion and more even distribution of Cr doping ions inside the ZGO host and, at the same time, lowers surface defect density to eliminate non-radiative pathway sources.

The PL emission spectra of the 60 mg weighed amount ZGOC CNCs, MSS-650 and HT-650 (Figure 3a) showed an intense NIR emission peak around 695 nm embedded with several fine features, which can be ascribed to $^2E \rightarrow {}^4A_2$ transition of trivalent $Cr^{3+}$ ions in an octahedral crystalline field.[53] This is consistent with the discussion on the XRD data that $Cr^{3+}$ dopants tend to occupy $Ga^{3+}$ sites in the ZGO host with distorted octahedral environment owing to their close ionic size matching.[54] The fine structures of the emission peaks are located around 661, 670, 681, 688, 696, 708 and 714 nm. The peak around 688 nm is the R-band ascribed to $Cr^{3+}$ ion in an unperturbed $O_h$ field. The one located at 696 nm is the N-band originated from $Cr^{3+}$ ion in the vicinity of zinc vacancy/interstitial pair ($V_{Zn}/Zn_i$) or antisite defects $Zn_{Ga}$' and $Ga_{Zn}{}^{o}$.[55,56,57] Among the other five fine peaks embedded in the major NIR peak around 659, 672, 679, 709 and 713 nm, the ones located at longer (709 and 713 nm) and shorter wavelengths (659, 672 and 679 nm) than 695 nm are known as Stoke's and anti-Stoke's phonon side bands, respectively.[53]

Moreover, the ZGOC MSS-650 and HT-650 NCs showed similar spectral features but higher emission intensities than the as-synthesized ZGOC CNCs. Such enhancement of PL emission output, and ultimately that of PersL intensity and duration, would be endowed by efficient thermal-driven diffusion and even distribution of dopant ions into the ZGO host lattice and reducing surface defects as undesirable non-radiative pathways by annealing at high temperature of 650°C.[58] The enhancement is very significant in both of the ZGOC MSS-650 and HT-650 NCs though that of the latter was slightly higher than that of the former. Inset of Figure 3a shows the digital images of the ZGOC CNCs, MSS-650 and HT-650 with identical mass under 256 nm irradiation. It can be clearly inferred from these images that the ZGOC MSS-650 NCs displayed bright red emission owing to the elimination of defects by thermal treatment and no light scattering due to the aggregate-free small sized particles.

The PL excitation spectra of the ZGOC CNCs, MSS-650 and HT-650 NCs under $\lambda_{em}$ = 695 nm (Figure S3) displayed three major peaks. The broad absorption band in the region of 225 – 325 nm peaking at 256 nm can be ascribed to the combination of host absorption and $O^{2-} \rightarrow Cr^{3+}$ charge transfer.[18,59] The other two excitation bands located at 410 and 560 nm would be attributed to $^4A_2 \rightarrow {}^4T_1$ and $^4A_2 \rightarrow {}^4T_2$ transitions arising from intra-configurational d-d electronic transitions of trivalent $Cr^{3+}$ ion.

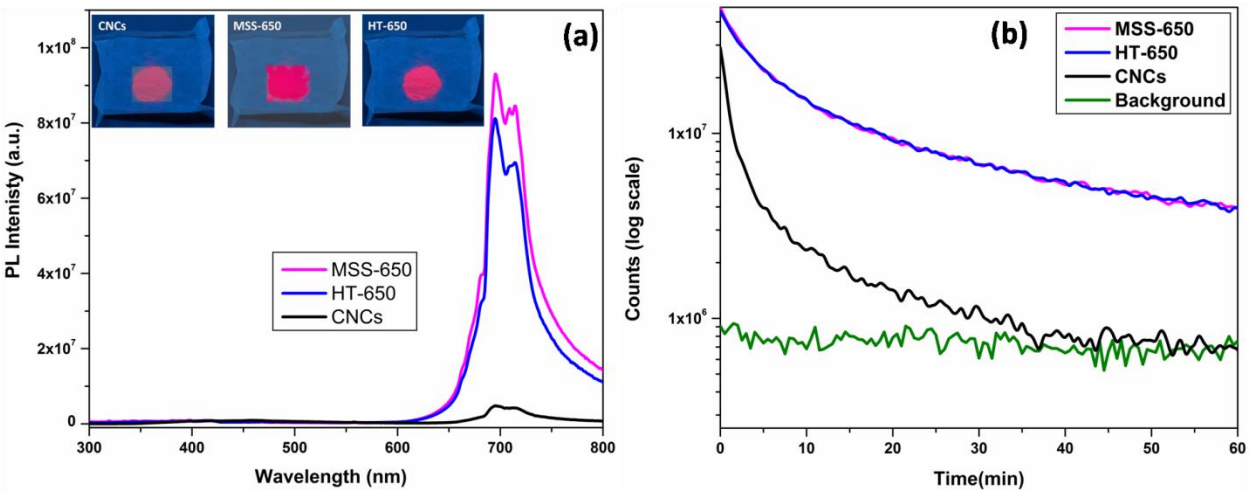


**Figure 3.** Optical properties of the ZGOC CNCs, MSS-650, and HT-650 NCs with the same amount of samples: (a) PL emission spectra with the insets showing their digital images (identical amount) under 256 nm irradiation. (b) PersL decay curves.

The NIR PersL decay curves of the ZGOC CNCs, MSS-650 and HT-650 NCs (Figure 3b) demonstrated continuous light emission up to 1 hr upon excitation with UV light at 256 nm for 5 min. Similar to the PL emission trend observed from these three samples (Figure 3a), the PersL intensity from the thermally treated MSS-650 and HT-650 NCs was much higher than that of the ZGOC CNCs. The proposed PersL mechanism of the ZGOC NCs showed in Figure S4 proceeds through four fundamental steps: (1) $Cr^{3+}$ excitation, (2) charge separation and trapping, (3) thermal detrapping of electron–hole pairs and capture by $Cr^{3+}$, and (4) $Cr^{3+}$ emission. The mechanism is similar to what has been discussed previously.[20,53]

After the excitation, conduction band electrons get trapped at singly ionized oxygen vacancy $V_O^{\blacksquare}$ / $Ga_{Zn}^{\blacksquare}$ defect states which act as electron traps and valence band holes get trapped inside antisite $Zn'_{Ga}$ defect states which act as hole traps (Step 2). Several defects present on the edges and interfaces of the CNCs also act as trap centers and help in the PersL process of the ZGOC NCs. The PersL mechanism for these ZGOC NCs involved the detrapping-trapping of electron-hole pairs positioned in the vicinity of $Cr^{3+}$doping ions and was triggered by the extent of cationic disorder in the ZGO host.

Step 3 is very important to understand why the thermal annealing treatment of the ZGOC CNCs led to enhancement of the PersL intensity of the MSS-650 and HT-650 NCs (Figure 3b). The extent

of PersL enhancement is the same in both these cases unlike their PL intensity where the HT-650 NCs had a slight edge. Such PersL enhancement can be ascribed to efficient de-trapping of electron–hole pairs which are captured by $Cr^{3+}$ and finally with high probability of $Cr^{3+}$ NIR emission. It is needed to be understood here that ultimately PersL intensity depends on trap density, electron capture cross-section of traps, emitting centers, and intensity of excitation light. PersL intensity actually varies following equation 1 below:[60]

$$I(t) = \frac{I_0}{(1+\gamma t)^n}(1) \qquad (1)$$

where $\gamma = \frac{N}{an_t}$ and $n$ = 0.5-2, $N$ = concentration of traps, $a$ = probability/sec for a trapped electron to be thermally excited into conduction band and $n_t$ = number of electrons per unit volume in traps. In our study here, the thermal annealing led to increase in trap density as well as thereby PersL improvement as per equation 1 was achieved. It is needed to be emphasized here that with annealing, crystallinity of the samples also increased and crystalline samples are expected to have relative less traps. In the literature, there are numerous reports wherein crystalline samples were found to have ample amount of traps. Dicks *et al.* did theoretical modeling of charge trapping in crystalline and amorphous $Al_2O_3$.[61] Schrek *et al.* recently showed high magnitude of traps to be present in single crystals as well.[62] Actually with increase in thermal annealing of our samples, both trap density and doping efficiency increased. Efficiency of chromium incorporated inside host lattice of ZGOC NCs would be meagered compared to the annealed samples as observed in our earlier work.[7]

We have also fitted the afterglow decay curves using exponential functions as explained by Tsai et al.[63] The results for the ZGOC CNCs, HT-650 and MSS-650 NCs are shown in Figures S5a-c along with the fitting equations and parameters. The decay constants are a means to determine decay rate of rapid, medium, and slow exponential decay components. The single exponential equation for the ZGOC CNCs and double exponential equations for the HT-and MSS-650 NCs that were fitted the experimental decay curves may correspond to one or two trap centers in the assumed models.

Traditionally the most prevalent way to improve PL intensity in nanophosphors is to coat them making core-shell nanoparticles with phosphors in the core and/or treating them at high temperature for a long time. This strategy is expected to increase PL intensity as it can take care of surface defects which are known as fluorescence quencher by providing non-radiative pathways. We also have tried several other strategies intended to improve the PL intensity, PersL intensity

and duration for the ZGOC CNCs. The first one involved thermal annealing and growth of the ZGOC CNCs at 300ºC for long enough time (e.g. 5 minutes *vs.*30 minutes) during the colloidal synthesis. However, this strategy was limited to enhance the PL to a reasonable QY of the ZGOC CNCs but not much improvement in terms of its PersL performance (Figure S6).

The second strategy was by overcoating of the ZGOC CNCs as the core to generate ZGOC@ZGO core-shell nanoparticles by adding extra Zn and Ga precursors at 250ºC to form a ZGO shell over the core of ZGOC CNCs. However, we observed improved PL emission (Figure S7a) but not enhanced PersL performance (Figure S7b).

We also heterogeneously overcoated the surface of the ZGOC CNCs by a $NaYF_4$ shell to grow heterogeneous ZGOC@$NaYF_4$ core-shell nanoparticles (Figure S8a). The TEM image clearly showed the formation of ZGOC@$NaYF_4$ core-shell nanoparticles. The average diameter of the core-shell nanoparticle is around 13.5 nm. The formation of these core-shell nanoparticles resulted in significant improvement of NIR PL emission intensity (Figure S8b). However, it did not improve the PersL intensity and duration (Figure S8c). In one of our recent work for ZGOC NCs, we reported that the use of a urea assisted hydrothermal method produced ZGOC NCs which showed remarkable enhancement in both PL and PersL compared to those NPs precipitated with ammonia or sodium hydroxide. We also reported that adding ammonium nitrate with urea led to the formation of ZGOC-ZnO core-shell NPs with further enhanced PL and PersL performance.[2,20] In all the above-mentioned comparison of PL emission, the spectra were normalized.

Although the ZGOC HT-650 and MSS-650 NCs showed comparable PL and PersL performance, the commercial viability for bioimaging and display applications of the former is poorer due to the aggregation formation of the NCs as seen in the TEM images (Figure 2c). For biomedical applications, the size of NCs should be as small as possible to enhance their cellular uptake. This requirement showed the superiority of the molten salt assisted annealing process of the ZGOC CNCs for not leading to any aggregation formation of the NCs while improving both the PL and PersL properties substantially. Therefore, we believe the molten salt assisted annealing process can be a game changer for PersL phosphors, especially their NCs for biomedical applications relying on intense fluorescence for invitro and *in vivo* imaging.

## Conclusion

ZGOC CNCs with low PL and PersL intensity limited their scientific investigation and commercial usage in information storage, display devices and bioimaging. In this study, we thermally annealed pre-formed ZGOC CNs in a molten salt medium (MSS-650) and observed enhancement in both PL and PersL (duration and intensity) without losing any advantages of the original CNCs such as monodispersity, sub-10 nm size and no-agglomeration. Exposing the pre-formed ZGOC CNCs to high temperature at ~650$^{o}$C (HT-650) though led improvement in both PL and PersL but caused the formation of aggregates. We were also successful in improving the PL intensity of ZGOC CNCs with three different strategies: (i) thermal annealing, (ii) overcoating, and (iii) core-shell strategy, but we yet achieved improvement in PersL intensity and duration. The work throws fascinating results wherein NCs were confined using molten salt assisted annealing which led to quenching of surface defects without the formation of any aggregates. At the same time, sonicating the ZGOC MSS-650 NCs made them water dispersible which is again an essential component of bioimaging. We believe the ZGOC NCs assisted with the molten salt confined treatment being sub-10 nm, biocompatible and aggregate-free and with much improved PL and PersL possess an extraordinary credential to be used in commercial market for bioimaging. Future works will be using this material for actual bioimaging experiments.

## ■ ASSOCIATED CONTENT

**Supporting Information:** The Supporting Information consisted of: Colloidal synthesis setup, schematic of molten salt confinement, PL emission spectra of ZGOC CNCs annealed for different duration, ZGO overcoated ZGOC NCs, ZGOC@$NaYF_4$ core-shell NPs, PL excitation spectra of ZGOC CNCs, MSS-650 and HT-650, and proposed mechanism of PersL in ZGOC.

## ■ AUTHOR INFORMATION

**Corresponding Author**: ymao17@iit.edu (YM)

**ORCID**

Bhupendra B. Srivastava: 0000-0002-9881-9502

Santosh K. Gupta: 0000-0002-1178-0159

Yuanbing Mao: 0000-0003-2665-6676

## Notes

The authors declare no competing financial interest.


## Acknowledgement

YM would like to thank the support by the National Science Foundation under CHE (award #1952803 and #1710160) and the IIT startup funds. SKG thanks the United States-India Education Foundation (USIEF) and the Institute of International Education (IIE) for his Fulbright Nehru Postdoctoral Fellowship (Award#2268/FNPDR/2017).


## References:


[1] T. Maldiney, A. Bessière, J. Seguin, E. Teston, S.K. Sharma, B. Viana, A.J.J. Bos, P. Dorenbos, M. Bessodes, D. Gourier, D. Scherman, C. Richard, *Nat. Mater.* **2014**, *13*, 418.

[2] Z. Li, Y. Zhang, X. Wu, L. Huang, D. Li, W. Fan, G. Han, *J. Am. Chem. Soc.* **2015**, *137*, 5304-5307.

[3] B.B. Srivastava, A. Kuang, Y. Mao, *Chem. Commun.* **2015**, *51*, 7372-7375.

[4] H. Tan, T. Wang, Y. Shao, C. Yu, L. Hu, *Front. Chem.* **2019**, *7*, 387.

[5] Z. Xue, X. Li, Y. Li, M. Jiang, H. Liu, S. Zeng, J. Hao, *ACS Appl. Mater. & Interfaces* **2017**, *9*, 22132-22142.

[6] B.B. Srivastava, S.K. Gupta, Y. Mao, *CrystEngComm* **2020**, *22*, 2491-2501.

[7] B.B. Srivastava, S.K. Gupta, Y. Mao, *J. Mater. Chem. C* **2020**, *8*, 6370-6379.

[8] R. Barbosa, S.K. Gupta, B.B. Srivastava, A. Villarreal, H. De Leon, M. Peredo, S. Bose, K. Lozano, *J. Lumin.* **2020**, *231*, 117760.

[9] Z. Wang, C.-Y. Zhu, S.-Y. Yin, Z.-W. Wei, J.-H. Zhang, Y.-N. Fan, J.-J. Jiang, M. Pan, C.-Y. Su, *Angew. Chem. Int. Ed.* **2019**, *58*, 3481-3485; *Angew. Chem.* **2019**, *131*, 3519-3523.

[10] Y. Jiang, Y. Li, C. Richard, D. Scherman, Y. Liu, *J. Mater. Chem. B* **2019**, *7*, 3796-3803.

[11] M.N. da Silva, J.M. de Carvalho, M.C. de Abreu Fantini, L.A. Chiavacci, C. Bourgaux, *ACS Appl. Nano Materials* **2019**, *2*, 6918-6927.

[12] M. Allix, S. Chenu, E. Véron, T. Poumeyrol, E.A. Kouadri-Boudjelthia, S. Alahraché, F. Porcher, D. Massiot, F. Fayon, *Chem. Mater.* **2013**, *25*, 1600-1606.

[13] L. Qin, P. Yan, C. Xie, J. Huang, Z. Ren, X. Li, S. Best, X. Cai, G. Han, *Nanoscale* **2018**, *10*, 13432-13442.

[14] L. Song, P.P. Li, W. Yang, X.H. Lin, H. Liang, X.F. Chen, G. Liu, J. Li, H.H. Yang, *Adv. Funct. Mater.* **2018**, *28*, 1707496.

[15] H.-F. Wang, X. Chen, F. Feng, X. Ji, Y. Zhang, *Chem. Sci.* **2018**, *9*, 8923-8929.

[16] Z. Li, Y. Zhang, X. Wu, X. Wu, R. Maudgal, H. Zhang, G. Han, *Adv. Sci.* **2015**, *2*, 1500001.

[17] B.B. Srivastava, S.K. Gupta, Y. Li, Y. Mao, *Dalton Trans.* **2020**, *49*, 7328-7340.

[18] A. Abdukayum, J.-T. Chen, Q. Zhao, X.-P. Yan, *J. Am. Chem. Soc.* **2013**, *135*, 14125-14133.

[19] T. Lecuyer, E. Teston, G. Ramirez-Garcia, T. Maldiney, B. Viana, J. Seguin, N. Mignet, D. Scherman, C. Richard, *Theranostics* **2016**, *6*, 2488.

[20] Z. Pan, Y.-Y. Lu, F. Liu, *Nat. Mater.* **2011**, *11*, 58.

[21] Y. Zhuang, J. Ueda, S. Tanabe, *Appl. Phys. Exp.* **2013**, *6*, 052602.

[22] A. Tuerdi, A. Abdukayum, *RSC Adv.* **2019**, *9*, 17653-17657.

[23] H.-X. Zhao, C.-X. Yang, X.-P. Yan, *Nanoscale* **2016**, *8*, 18987-18994.

[24] Z. Hu, D. Ye, X. Lan, W. Zhang, L. Luo, Y. Wang, *Opt. Mater. Exp.* **2016**, *6*, 1329-1338.

[25] M.K. Hussen, F.B. Dejene, *J. Sol-Gel Sci. & Tech.* **2018**, *88*, 454-464.

[26] T. Luan, J. Liu, X. Yuan, J.-G. Li, *Nanoscale Res. Lett.* **2017**, *12*, 219.

[27] L. Liu, S. Hu, Y. Wang, S. Yang, J. Qu, *Sci. Rep.* **2018**, *8*, 8866.

[28] R. Zou, J. Huang, J. Shi, L. Huang, X. Zhang, K.-L. Wong, H. Zhang, D. Jin, J. Wang, Q. Su, *Nano Research* **2017**, *10*, 2070-2082.

[29] J. Shi, X. Sun, J. Zhu, J. Li, H. Zhang, *Nanoscale* **2016**, *8*, 9798-9804.

[30] E. Teston, S. Richard, T. Maldiney, N. Lièvre, G.Y. Wang, L. Motte, C. Richard, Y. Lalatonne, *Chem.– A Eur. J.* **2015**, *21*, 7350-7354.

[31] S. Jana, B.B. Srivastava, N. Pradhan, *J. Phys. Chem. C* **2013**, *117*, 1183-1188.

[32] X. Peng, J. Wickham, A. Alivisatos, *J. Am. Chem. Soc.* **1998**, *120*, 5343-5344.

[33] Z.A. Peng, X. Peng, *J. Am. Chem. Soc.* **2001**, *123*, 1389-1395.

[34] B.B. Srivastava, S. Jana, D. Sarma, N. Pradhan, *J. Phys. Chem. Lett.* **2010**, *1*, 1932-1935.

[35] P.D. Howes, R. Chandrawati, M.M. Stevens, *Science* **2014**, *346*, 1247390.

[36] D. Nykypanchuk, M.M. Maye, D. van der Lelie, O. Gang, *Nature* **2008**, *451*, 549.

[37] V. Srivastava, V. Kamysbayev, L. Hong, E. Dunietz, R.F. Klie, D.V. Talapin, *J. Am. Chem. Soc.* **2018**, *140*, 12144-12151.

[38] H. Zhang, K. Dasbiswas, N.B. Ludwig, G. Han, B. Lee, S. Vaikuntanathan, D.V. Talapin, *Nature* **2017**, *542*, 328.

[39] H.-J. Byun, J.-U. Kim, H. Yang, *Nanotech.* **2009**, *20*, 495602.

[40] M. Cao, I. Djerdj, M. Antonietti, M. Niederberger, *Chem. Mater.* **2007**, *19*, 5830-5832.

[41] M.A. Penilla Garcia, S.K. Gupta, Y. Mao, *Ceram. Intern.* **2020**, *46*, 1352-1361.

[42] X. Liu, N. Fechler, M. Antonietti, *Chem. Soc. Rev.* **2013**, *42*, 8237-8265.

[43] S.K. Gupta, Y. Mao, *Prog. Mater. Sci.* **2020**, *117*, 100734.

[44] F. Gonell, C.M. Sánchez-Sánchez, V. Vivier, C. Laberty-Robert, D. Portehault, *ACS Appl. Nano Mater.* **2020**, *3*, 7482-7489.

[45] B. Li, D. Zhang, G. Li, J. Fan, D. Chen, Y. Ge, L. Li, *Chem. – A Eur. J.* **2019**, *25*, 2003-2010.

[46] G. Huang, X. Du, F. Zhang, D. Yin, L. Wang, *Chem. – A Eur. J.* **2015**, *21*, 14140-14145.

[47] M. Pokhrel, S.K. Gupta, K. Wahid, Y. Mao, *Inorg. Chem.* **2019**, *58*, 1241-1251.

[48] T. van Westen, R.D. Groot, *Crystal Growth & Design* **2018**, *18*, 4952-4962.

[49] J.N. Israelachvili, *Intermolecular and surface forces*, Academic press, 2011.

[50] B. Deraguin, L. Landau, *Acta Physicochim: USSR* **1941**, *14*, 633-662.

[51] E.J.W. Verwey, J.T.G. Overbeek, K. Van Nes, *Theory of the stability of lyophobic colloids: the interaction of sol particles having an electric double layer*, Elsevier Publishing Company, 1948.

[52] O.J. Lanning, P.A. Madden, *J. Phys. Chem. B* **2004**, *108*, 11069-11072.

[53] A. Bessière, S.K. Sharma, N. Basavaraju, K.R. Priolkar, L. Binet, B. Viana, A.J.J. Bos, T. Maldiney, C. Richard, D. Scherman, D. Gourier, *Chem. Mater.* **2014**, *26*, 1365-1373.

[54] H. Kahan, R. Macfarlane, *J. Chem. Phys.* **1971**, *54*, 5197-5205.

[55] W. Nie, F.M. Michel-Calendini, C. Linarès, G. Boulon, C. Daul, *J. Lumin.* **1990**, *46*, 177-190.

[56] W. Zhang, J. Zhang, Z. Chen, T. Wang, S. Zheng, *J. Lumin.* **2010**, *130*, 1738-1743.

[57] N. Basavaraju, K.R. Priolkar, D. Gourier, S.K. Sharma, A. Bessière, B. Viana, *Phys. Chem. Chem. Phys.* **2015**, *17*, 1790-1799.

[58] S.K. Gupta, J.P. Zuniga, M. Abdou, Y. Mao, *Inorg. Chem. Front.* **2018**, *5*, 2508-2521.

[59] Y. Wang, C.-X. Yang, X.-P. Yan, *Nanoscale* **2017**, *9*, 9049-9055.

[60] S. Shionoya, W.M. Yen, H. Yamamoto, *Phosphor Handbook*, CRC press, 2018.

[61] O.A. Dicks, A.L. Shluger, *J. Phys.: Condensed Matter* **2017**, *29*, 314005.

[62] M. Schreck, P. Ščajev, M. Träger, M. Mayr, T. Grünwald, M. Fischer, S. Gsell, *J. Appl. Phys.* **2020**, *127*, 125102.

[63] C.-Y. Tsai, J.-W. Lin, Y.-P. Huang, Y.-C. Huang, *Modeling and Assessment of Long Afterglow Decay Curves*, The Scientific World Journal *2014*, 102524.

**TOC:**

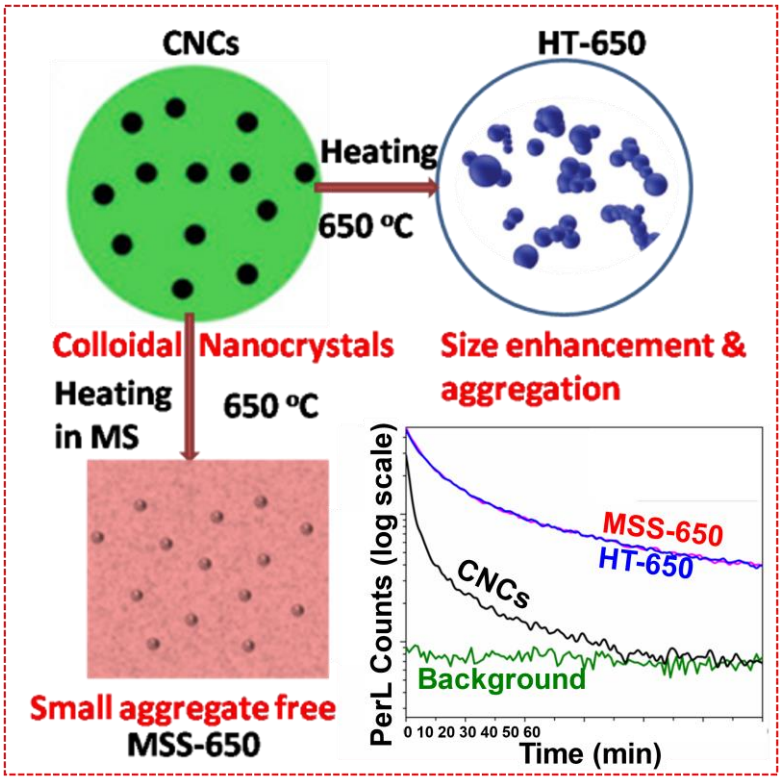


New concept on molten salt confinement to thermally anneal as-synthesized sub-10 nm $ZnGa_2O_4:Cr^{3+}$ (ZGOC) colloidal nanocrystals in a molten salt media at 650°C for improving their persistent luminescence (PersL) intensity and lifetime without losing their nanostructural characteristics, water dispersibility and biocompatibility.